AMERICAN SOCIETY FOR MICROBIOLOGY | Journal of Virology®

PATHOGENESIS AND IMMUNITY

Assessing the Protective Potential of H1N1 Influenza Virus Hemagglutinin Head and Stalk Antibodies in Humans

Shannon R. Christensen,[a] Sushila A. Toulmin,[a] Trevor Griesman,[a] Lois E. Lamerato,[b] Joshua G. Petrie,[c] Emily T. Martin,[c] Arnold S. Monto,[c] Scott E. Hensley[a]

[a]Department of Microbiology, Perelman School of Medicine, University of Pennsylvania, Philadelphia, Pennsylvania, USA
[b]Department of Public Health Sciences, Henry Ford Health System, Detroit, Michigan, USA
[c]Department of Epidemiology, University of Michigan School of Public Health, Ann Arbor, Michigan, USA

ABSTRACT Seasonal influenza viruses are a major cause of human disease worldwide. Most neutralizing antibodies (Abs) elicited by influenza viruses target the head domain of the hemagglutinin (HA) protein. Anti-HA head Abs can be highly potent, but they have limited breadth since the HA head is variable. There is great interest in developing new universal immunization strategies that elicit broadly neutralizing Abs against conserved regions of HA, such as the stalk domain. Although HA stalk Abs can provide protection in animal models, it is unknown if they are present at sufficient levels in humans to provide protection against naturally acquired influenza virus infections. Here, we quantified H1N1 HA head- and stalk-specific Abs in 179 adults hospitalized during the 2015–2016 influenza virus season. We found that HA head Abs, as measured by hemagglutinin inhibition (HAI) assays, were associated with protection against naturally acquired H1N1 infection. HA stalk-specific serum total IgG titers were also associated with protection, but this association was attenuated and not statistically significant after adjustment for HA head-specific Ab titers. We found slightly higher titers of HA stalk-specific IgG1 and IgA Abs in sera from uninfected participants than in sera from infected participants; however, we found no difference in serum *in vitro* antibody-dependent cellular cytotoxicity activity. In passive transfer experiments, sera from participants with high HAI activity efficiently protected mice, while sera with low HAI activity protected mice to a lower extent. Our data suggest that HA head Abs are more efficient at protecting against H1N1 infection than HA stalk Abs.

IMPORTANCE Abs targeting the HA head of influenza viruses are often associated with protection from influenza virus infections. These Abs typically have limited breadth, since mutations frequently arise in HA head epitopes. New vaccines targeting the more conserved HA stalk domain are being developed. Abs that target the HA stalk are protective in animal models, but it is unknown if these Abs exist at protective levels in humans. Here, we completed experiments to determine if Abs against the HA head and stalk were associated with protection from naturally acquired human influenza virus infections during the 2015–2016 influenza season.

KEYWORDS antibody function, antibody repertoire, influenza

Seasonal influenza viruses cause annual epidemics worldwide. Although seasonal influenza vaccines usually provide moderate protection against circulating strains, vaccine effectiveness can be low when there are antigenic mismatches between vaccine strains and circulating strains (1, 2). Additionally, rare yet unpredictable influenza pandemics occur when novel influenza virus strains cross the species barrier and transmit in the human population (3).

Antibody (Ab)-mediated immunity is important for protecting against influenza

Citation Christensen SR, Toulmin SA, Griesman T, Lamerato LE, Petrie JG, Martin ET, Monto AS, Hensley SE. 2019. Assessing the protective potential of H1N1 influenza virus hemagglutinin head and stalk antibodies in humans. J Virol 93:e02134-18. https://doi.org/10.1128/JVI.02134-18.

Editor Mark T. Heise, University of North Carolina at Chapel Hill

Address correspondence to Scott E. Hensley, hensley@pennmedicine.upenn.edu.

Received 29 November 2018
Accepted 23 January 2019
Accepted manuscript posted online 30 January 2019
Published 3 April 2019

virus infections (4). The viral membrane protein, hemagglutinin (HA), is the target for most anti-influenza virus neutralizing Abs (5–9). Most neutralizing HA Abs target the HA globular head domain and block virus attachment to sialic acid, the cellular receptor for influenza viruses. However, since the HA head is highly variable, HA head Abs generally exhibit poor cross-reactivity against antigenically drifted viral strains (10). Unlike the head domain, the stalk domain of HA is highly conserved between different influenza virus strains. Abs that target the HA stalk domain can prevent viral replication by inhibiting the pH-induced conformational changes of HA that are required for viral entry into the cell (11). Many HA stalk-specific Abs also protect by blocking HA maturation (11), inhibiting viral egress (12), or mediating Ab-dependent cellular cytotoxicity (ADCC) (13). Although HA stalk Abs are typically subdominant and are not thought to be as efficient as HA head Abs, HA stalk Abs can inhibit diverse influenza strains *in vitro* (14–17).

Conventional influenza vaccines effectively elicit HA head-reactive Abs but not HA stalk Abs (18). As a result, influenza vaccine effectiveness is dependent on the similarity of the HA head of circulating influenza virus strains and the HA head of vaccine strains (19). Antigenic mismatch between influenza vaccine strains and circulating viral strains have been especially problematic during recent years (20, 21). To circumvent the potential for antigenic mismatch, as well as to prepare against new pandemic viral strains, there is great interest in developing new universal immunization strategies that elicit broadly reactive Abs against conserved regions of HA, such as the stalk domain (22).

HA stalk Abs protect animals from group 1 and group 2 influenza A virus infections (14, 16, 23–29). For example, human anti-HA stalk monoclonal Abs (MAbs) protect mice from lethal pH1N1 infection following prophylactic or therapeutic passive transfers (23, 28) as well as against H5N1 (16, 24, 28) or H7N9 lethal dose challenge (27). Both the prophylactic passive transfer of a human anti-HA stalk MAb or the elicitation of HA stalk-specific Abs by chimeric HA vaccination decreases viral loads in ferrets following pH1N1 infection (25). Additionally, passive transfer of human sera from H5N1 vaccinees protects mice from lethal pH1N1 infection (26), and this protection is likely mediated by HA stalk Abs. Passive transfer of broadly neutralizing HA stalk-specific MAbs against group 2 influenza A viruses also protects mice against heterosubtypic H3 viruses (29) and heterologous H3 and H7 viruses (14). Vaccine strategies designed to elicit HA stalk Abs in humans are currently being pursued (30–32). These strategies include sequential immunizations with chimeric HAs (19, 33), immunization with headless HA antigens (30, 34, 35), and immunizations with mRNA-based vaccines expressing HA (32).

Despite the recent interest in developing new HA stalk-based vaccines, the amount of HA stalk Abs required to protect humans from influenza virus infections and influenza-related disease has not been established. A recent human pH1N1 challenge study demonstrated that HA stalk Ab titers are associated with reduced viral shedding but are not independently associated with protection against influenza infection (36). While human influenza virus challenge studies are valuable, they have some limitations. For example, high doses of virus are used in these studies (37, 38), large numbers of individuals are typically prescreened for certain immunological attributes prior to entering these studies (39), and the pathogenesis of infection differs from that of a natural infection, including key sites of viral replication (38, 40). Serological studies of individuals who naturally acquire influenza virus infections can also be used to identify specific types of Abs that are associated with protection. Here, we present a serological study to determine if serum HA head and stalk Abs are associated with protection against naturally acquired H1N1 infection.

(This article was submitted to an online preprint archive [41].)

RESULTS

Assessment of HA head and stalk Ab association with protection against H1N1 infection. We analyzed sera collected from 179 participants enrolled in a hospital-based study during the 2015–2016 influenza season (Table 1). Adults hospitalized at the

TABLE 1 Demographic characteristics of subjects enrolled in hospital-based human cohort study

Parameter[a]	No. (%) of cases[b]	
	H1N1 infected	H1N1 uninfected
Age		
18–49 yr	24 (38.7)	43 (36.8)
50–64 yr	21 (33.9)	39 (33.3)
≥65 yr	17 (27.4)	35 (29.9)
Vaccination status		
Vaccinated	27 (43.5)	57 (48.7)
Unvaccinated	35 (56.5)	60 (51.3)
Sex		
Male	30 (48.4)	66 (56.4)
Female	32 (51.6)	51 (43.6)
Race		
White	35 (56.5)	61 (53.5)
Black	20 (32.3)	37 (31.6)
Other/Unknown	7 (11.3)	19 (16.2)
Days from illness onset to blood collection		
≤3 days	41 (69.5)	60 (52.6)
>3 days	18 (30.5)	54 (47.4)

[a]Cases and controls were matched for age group and vaccination status.
[b]Shown are the number and percentage of each demographic characteristic within the infected and uninfected groups.

University of Michigan Hospital (Ann Arbor, MI, USA) or Henry Ford Hospital (Detroit, MI, USA) were enrolled according to a case definition of within ≤10 days of acute respiratory illness onset and subsequently tested for influenza by reverse transcription-PCR (RT-PCR). Serum specimens collected at hospital admission were obtained for estimation of preinfection/early infection antibodies; 58% of specimens included in this analysis were collected within 3 days of illness onset (42). We analyzed serum samples from 62 hospitalized individuals that had PCR-confirmed H1N1 influenza virus infections. Serum samples from 117 controls were selected from hospitalized individuals that had other respiratory diseases not caused by an influenza virus infection, matching by age category (18 to 49 years, 50 to 64 years, and ≥65 years) and influenza vaccination status.

We quantified serum titers of HA head-specific Abs against the predominant 2015–2016 H1N1 strain using hemagglutination inhibition (HAI) assays (Fig. 1A). HAI assays detect HA head-specific Abs that prevent influenza virus-mediated cross-linking of red blood cells (43, 44). We found that HAI titers were associated with protection against H1N1 infection in logistic regression models (Table 2). We observed a 23.4% reduction in H1N1 infection risk with every 2-fold increase in HAI titer. Previous studies reported that a 1:40 HAI titer is associated with 50% protection from experimental human influenza infections (45). Consistent with this, over 21% of non-H1N1-infected cases possessed an HAI titer of >40, while only ~3% of H1N1-infected cases possessed an HAI titer of >40.

We next quantified relative titers of H1 stalk IgG Abs using enzyme-linked immunosorbent assays (ELISAs) coated with headless H1 proteins (Fig. 1B). Similar to HAI titers, we found that H1 stalk titers were associated with protection against H1N1 infection in logistic regression models (Table 2). We observed a 14.2% reduction in H1N1 infection risk with every 2-fold increase in H1 stalk titer. Whereas HAI titers of >40 were sharply associated with protection (Fig. 1A and C), there was no clear HA stalk IgG titer cutoff that was associated with protection in our study (Fig. 1B and C). Samples with the highest HA stalk IgG titers were interspersed among the uninfected and infected groups (Fig. 1B and C).

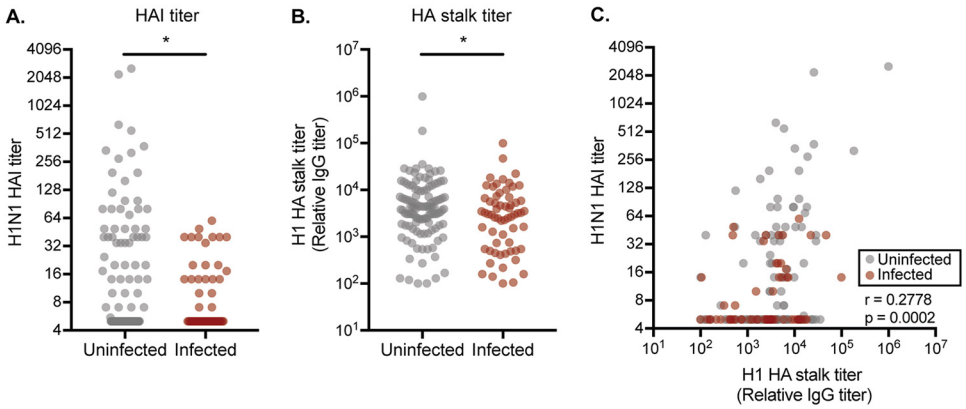

FIG 1 Assessment of HA head and stalk Ab association with protection. (A) HAI assays were completed using sera from uninfected (gray) and infected (red) individuals. HAI titers are associated with protection against H1N1 infection ($P = 0.0108$, logistic regression of $\log_2$ geometric mean titers from two independent experiments). (B) ELISAs using headless HA constructs were completed using sera from uninfected (gray) and infected (red) individuals. HA stalk-specific Abs are associated with protection against influenza infection ($P = 0.0417$, logistic regression analysis using $\log_2$ geometric mean titers from two independent experiments). (C) HA head Abs measured by HAI and HA stalk titers measured by ELISA using headless HA stalk constructs are weakly, though significantly, correlated ($r = 0.2778$, $P = 0.0002$, Spearman correlation using $\log_2$ geometric mean titers from two independent experiments for each measurement). In all panels, each circle represents a serum sample from a single individual.

Although both HAI titers and HA stalk IgG titers were associated with H1N1 protection in unadjusted models (Table 2), only HAI titers remained statistically associated with protection in adjusted models (Table 2). HA stalk IgG-associated protection lost significance when adjusting for HAI titers; however, the overall reduction in odds of infection for each 2-fold increase in titer remained roughly the same between the unadjusted and adjusted models for both HAI (23.4% to 20.7%) and stalk Ab titers (14.2% to 9.8%), respectively (Table 2).

We completed several experiments to validate our HA stalk IgG data. Headless H1 proteins are engineered to possess only the HA stalk domain and not the HA globular head domain (30). We completed experiments with monoclonal Abs (MAbs) to verify that HA stalk-reactive Abs bind to headless H1 proteins in ELISAs. We found that the H1 head-specific EM-4C04 MAb bound efficiently to a full-length H1 HA protein but failed to bind to our headless H1 protein, while the H1 stalk-specific 70-1F02 MAb bound to each construct similarly (Fig. 2A and B). We used two additional methods to verify that headless HA-based ELISAs accurately quantify HA stalk-reactive Abs. First, we measured Ab binding to a full-length HA chimeric protein that possessed an exotic head domain from an H6 virus fused to the H1 stalk (abbreviated c6/H1) (46). Since H6 viruses have never circulated in the human population, most human Abs that bind to this recombinant HA target the HA stalk domain (19). We found similar relative HA stalk Ab levels when we used the c6/H1 HA-based ELISAs instead of headless HA-based ELISAs (Fig. 2C). We also quantified HA stalk Ab levels using a competition ELISA. For these experiments, we determined the amount of serum Abs that was required to prevent the

TABLE 2 Logistic regression modeling of HA head and stalk antibody association with protection[a]

	$\log_2$ titer *P* value, OR (95% CI)	
Model	**HAI**	**Stalk**
HAI only	0.0108, 0.766 (0.615, 0.928)	
Stalk only		0.0417, 0.858 (0.738, 0.992)
HAI + stalk	0.0318, 0.793 (0.632, 0.969)	0.1932, 0.902 (0.769, 1.053)

[a]Logistic regression analyses using both unadjusted (HAI only and stalk only) and adjusted (HAI plus stalk) models. Values represent $\log_2$ geometric mean titers from two independent experiments. OR, odds ratio; CI, confidence interval.

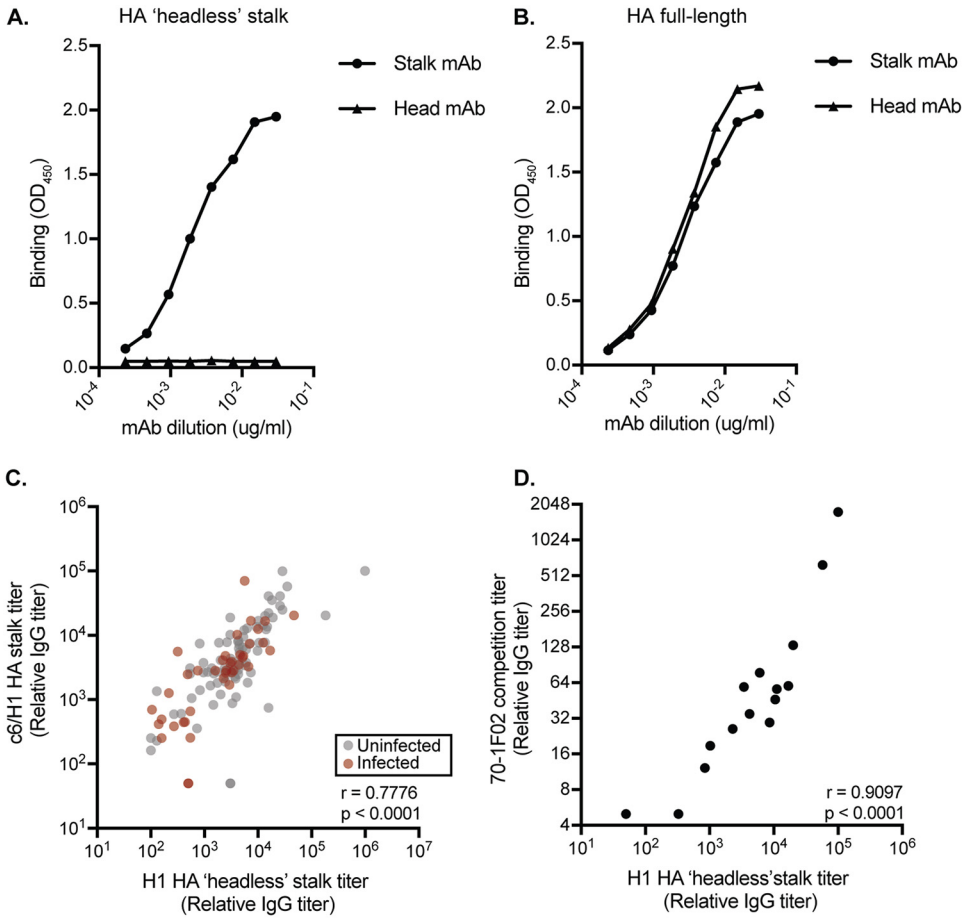

FIG 2 Validation of headless H1 HA stalk construct. We completed additional ELISAs using the 70-1F02 HA stalk MAb and the EM-4C04 HA head Ab and plates coated with headless HA (A) or full-length HA (B). Graphs depict representative results from two independent experiments. (C) We quantified HA stalk Abs using ELISA plates coated with c6/H1 proteins. HA stalk titers measured by ELISA using c6/H1 or headless HA stalk constructs were tightly correlated ($r = 0.7776$, $P < 0.0001$, Spearman correlation using $\log_2$ geometric mean titers from two independent experiments). (D) We completed competition assays using the conformationally dependent 70-1F02 MAb. 70-1F02 competition titers are tightly correlated with overall HA stalk Ab titers in both infected and uninfected individuals ($r = 0.9097$, $P < 0.0001$, Spearman correlation using $\log_2$ geometric mean titers from two independent experiments). In panels C and D, each circle represents a serum sample from a single individual.

binding of a biotinylated HA stalk-specific MAb (70-1F02). The 70-1F02 MAb recognizes a conformationally dependent epitope that spans the HA1 and HA2 subunits (15, 17, 28, 47, 48). We found that 70-1F02-based competition assay titers correlated strongly with the headless HA-based ELISA titers (Fig. 2D).

Assessment of HA stalk-specific serum Ab isotypes. Some HA stalk Abs mediate protection through nonneutralizing mechanisms that involve processes such as ADCC (49). IgG1 and IgG3 Ab subtypes are efficient at inducing ADCC, whereas IgG2 and IgG4 are not (50). We quantified relative IgG1, IgG2, and IgG3 HA stalk Abs in serum from a subset of participants using ELISAs coated with headless H1 proteins. In all participants, the majority of HA stalk IgGs were IgG1 (Fig. 3A), consistent with previous reports (51, 52). HA stalk IgG1 Ab titers were slightly higher in uninfected participants than in infected participants (Fig. 3A). Total HA stalk IgG titers closely correlated with HA stalk IgG1 titers (Fig. 3B). Undetectable levels of IgG2 and very low levels of IgG3 HA stalk Abs were detected in serum (Fig. 3A). We did not measure levels of IgG4 HA stalk Abs, since previous studies have shown that IgG4 is not prevalent among anti-influenza virus human Abs (51). It is important to note that titers of each isotype are directly comparable in our experiments, since we used control MAbs in each ELISA (based on

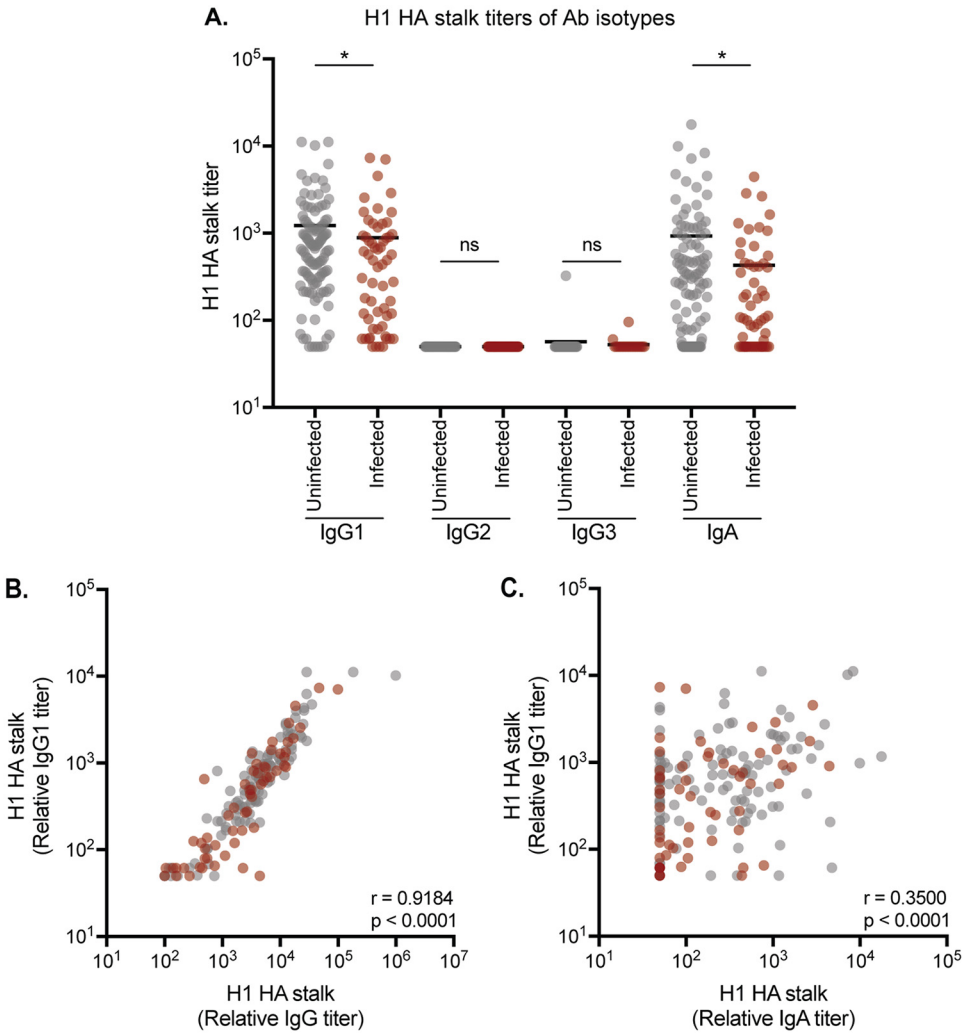

FIG 3 Assessment of HA stalk-specific serum Ab isotypes. (A) ELISAs were completed to quantify the levels of IgG1, IgG2, IgG3, and IgA HA stalk Abs in each serum sample. Higher titers of HA stalk-specific IgG1 and IgA were present in uninfected individuals but not in infected individuals ($P = 0.0180$ and $P = 0.0426$, respectively, by Welch's *t* test using $\log_2$-transformed mean titers from two independent experiments). (B) IgG1 HA stalk Ab titers closely correlated with total IgG HA stalk Ab titers ($r = 0.9184$, $P < 0.0001$, Spearman correlation using $\log_2$ geometric mean titers from two independent experiments). (C) IgA HA stalk Ab titers moderately correlated with IgG1 HA stalk Ab titers ($r = 0.3500$, $P < 0.0001$, Spearman correlation using $\log_2$ geometric mean titers from two independent experiments). In all panels, each circle represents a serum sample from a single individual.

the CR9114 HA stalk MAb [53, 54]) that were engineered to possess the same variable regions coupled to different constant regions.

We next evaluated serum HA stalk IgA Abs, since IgA Abs can be important for controlling respiratory infections. For example, mucosal IgA potently reduces the risk of influenza transmission events in guinea pigs in a dose-dependent manner (55) and suppresses the extracellular release of virus from infected cells (56). Further, anti-HA stalk MAbs engineered on an IgA backbone neutralize virus more effectively than when they are engineered on an IgG backbone (57). We did not have access to respiratory secretions, but we did measure levels of HA stalk monomeric IgA in the serum from a subset of participants. Similar to HA stalk IgG1 titers (Fig. 3A), we found that serum HA stalk IgA titers were slightly higher in uninfected participants than in infected participants (Fig. 3A). IgG1 and IgA titers were moderately, though significantly, correlated (Fig. 3C).

Functionality of Abs from infected and uninfected individuals. Abs against the HA head and HA stalk can neutralize or limit virus replication through distinct mech-

anisms (11–14, 47–49, 58, 59). For example, most Abs that target epitopes near the receptor binding domain of the HA head block virus binding and neutralize virus *in vitro* and *in vivo* (58). Some HA stalk Abs can directly neutralize virus, but the majority of HA stalk Abs require Fc receptor engagement for protection *in vivo* (15, 49, 60). Neutralizing HA stalk Abs typically inhibit HA conformational changes required to mediate fusion of the virus and cellular membranes (11, 14, 47, 48). Other HA stalk Abs can prevent subsequent viral expansion at later stages of infection by inhibiting HA maturation (11) and viral egress (12).

We completed experiments to assess the *in vitro* and *in vivo* protective potential of serum Abs from a subset of infected and uninfected individuals. First, we performed *in vitro* neutralization assays using green fluorescent protein (GFP)-reporter influenza viruses (61). We generated H1N1 viruses possessing genes encoding enhanced GFP (eGFP) in place of most of the PB1 gene segment. The eGFP segment retained the noncoding and 80 terminal coding nucleotides, allowing this segment to be efficiently and stably packaged into virions. Neutralization assays were completed with these viruses in cell lines that stably expressed PB1. We detected *in vitro* neutralization titers in serum from approximately half of the participants that we tested. We found that *in vitro* neutralization titers were significantly higher in the uninfected group than in the infected group by Welch's *t* test (Fig. 4A). As expected, serum samples with the highest HAI titers had high *in vitro* neutralization titers (Fig. 4B), whereas serum samples with the highest HA stalk titers had more variable *in vitro* neutralization titers (Fig. 4C).

We next completed *in vitro* ADCC assays using serum from a subset of participants. As controls, we also tested MAbs against the HA stalk (CR9114) and HA head (EM-4C04). For these assays, we incubated HA-expressing 293T cells with serum and then added human peripheral blood mononuclear cells (PBMCs). We then measured CD107a (LAMP1) expression on $CD3^-$ $CD56^+$ NK cells by flow cytometry. CD107a is a sensitive NK cell degranulation marker whose expression levels strongly correlate with cytokine production and cytotoxicity by NK cells in response to Ab-Fc receptor engagement (62). Consistent with previous studies (53), the CR9114 HA stalk MAb activated NK cells more efficiently than the EM-4C04 HA head MAb (Fig. 4D). Serum samples from participants also activated NK cells, but importantly, we found no differences between NK activation in sera from infected and that from uninfected individuals (Fig. 4D).

Finally, we completed passive transfer experiments in mice. For these experiments we passively transferred human sera into mice that have been engineered to possess human Fc receptors (63) so that we could accurately assess the protective effects mediated by human Fc-FcR interactions. We passively transferred pooled sera from uninfected individuals that had high (>40) HAI titers (abbreviated as uninfected HAI^{high}) and uninfected individuals that had low ($\leq$ 40) HAI titers (abbreviated as uninfected HAI^{low}). We also passively transferred pooled sera from infected individuals, all of whom had low ($\leq$ 40) HAI titers (abbreviated as infected HAI^{low}). For these experiments, equal volumes of human sera were transferred for each experimental condition. Mice were challenged with a sublethal dose of H1N1 4 h after serum transfer, and body weights were monitored for 15 days (Fig. 5A). Mice that received sera from uninfected HAI^{high} participants were fully protected against H1N1 infection. Mice that received sera from HAI^{low} participants, whether from uninfected or infected individuals, were moderately protected against H1N1 infection, although these sera conferred significantly less protection than sera from HAI^{high} participants (Fig. 5B and Table 3). Since there were different amounts of HA Abs in sera from uninfected HAI^{high} participants, uninfected HAI^{low} participants, and infected participants (Fig. 5C), it is unclear if the differences in our passive transfer experiments were due to differences in overall HA Ab titers or differences in HA head and stalk Ab ratios. To address this, we repeated passive transfer experiments after adjusting serum amounts so that equal amounts of HA Abs were passively transferred in each experimental group. Similar to what we found in our initial passive transfer experiment, sera from uninfected HAI^{high} participants protected mice better than sera from uninfected HAI^{low} participants and infected participants (Fig. 5D and Table 4). Interestingly, sera from uninfected HAI^{low} participants

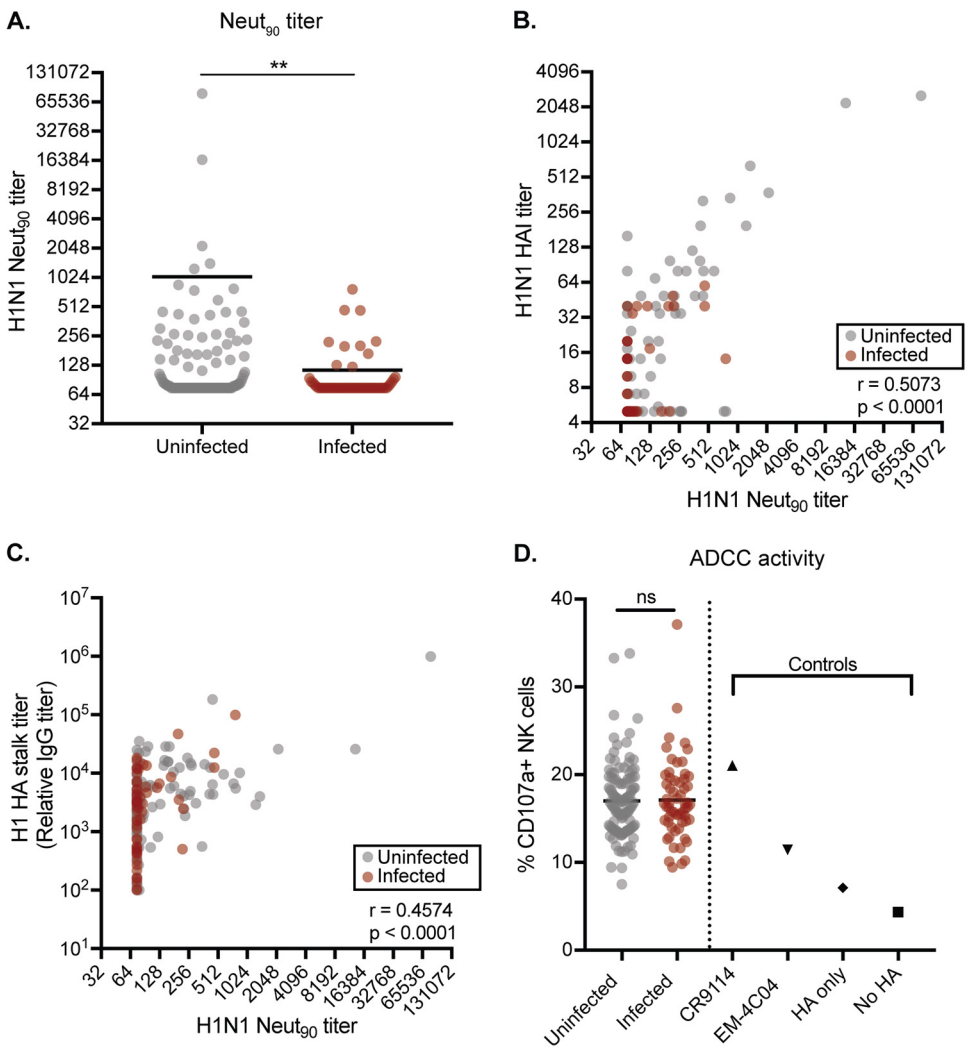

FIG 4 *In vitro* functionality of HA Abs from infected and uninfected individuals. (A) *In vitro* neutralization assays were completed with sera from uninfected and infected individuals. *In vitro* neutralization titers are significantly higher in uninfected than infected participants ($P = 0.0026$, Welch's t test using $\log_2$ mean titers from two independent experiments). Neut_{90}, neutralization titer at which the inverse of the highest dilution decreased mean fluorescence by 90% relative to infected control wells in the absence of antibodies. (B) HAI titers correlate strongly with neutralization titers ($r = 0.5073$, $P < 0.0001$, Spearman correlation using $\log_2$ geometric mean titers from two independent experiments). (C) HA stalk titers also correlate with neutralization titers ($r = 0.4574$, $P < 0.0001$, Spearman correlation using $\log_2$ geometric mean titers from two independent experiments). (D) ADCC assays were completed using sera from uninfected and infected individuals. Assays were also completed using the CR9114 and EM-4C04 MAbs. As negative controls, we completed ADCC assays using 293T cells without HA or 293T cells with HA but without Ab. ADCC activity is not significantly different between the uninfected and infected participants ($P = 0.9538$, Welch's t test using $\log_2$ mean titers from three independent experiments).

protected mice better than sera from infected participants after adjusting serum amounts based on HA Ab titers (Fig. 5D and Table 4). Taken together, these data suggest that human sera with high HAI activity efficiently protect *in vivo*, while human sera with low HAI activity also protect *in vivo*, albeit to a lower extent.

DISCUSSION

Observational studies can be useful in identifying Ab types that are associated with protection from influenza virus infection. Here, we found that both HA head and stalk Abs appeared to be associated with preventing H1N1 hospitalizations during the 2015–2016 season. We found that the effect size of HAI-associated protection (23.4% reduced risk of infection for every 2-fold increase in titer) was larger than the effect size of HA stalk Ab-associated protection (14.2% reduced risk of infection for every 2-fold

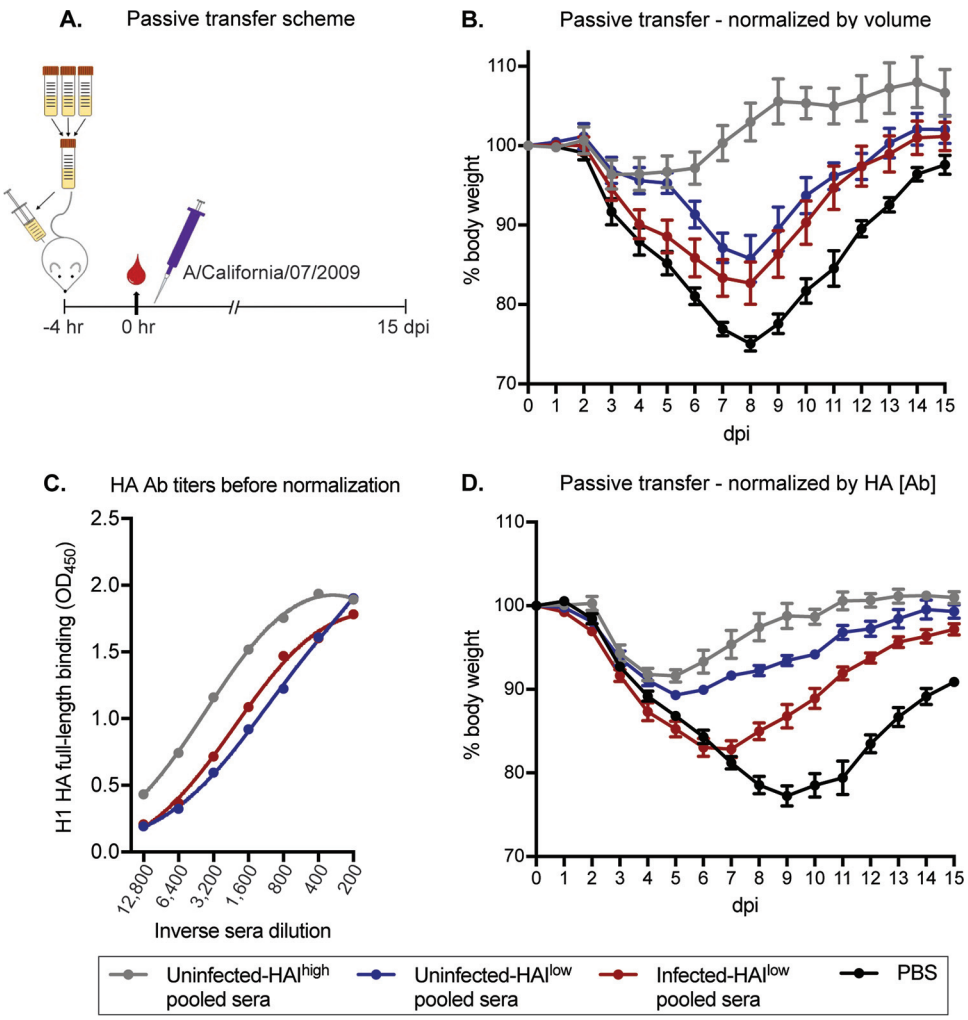

FIG 5 HA head and stalk antibodies confer protection from severe disease *in vivo*. (A) Passive transfer experiment design and timeline. Sera were stratified by HAI titer and infection status, pooled, and transferred intraperitoneally to humanized Fc-receptor mice 4 h before challenge with A/California/07/2009. Weights were measured daily for 15 days. (B) We transferred equal volumes of sera into each mouse for our initial experiments. Mice that received uninfected HAI^{high} sera were completely protected against infection (gray line). Mice that received HAI^{low} sera (uninfected or infected, blue and red lines, respectively) were also protected but were significantly less protected than the mice that received HAI^{high} sera (results are given with ± standard errors of the means [SEM]; 1-way ANOVA was performed for each day postinfection based on percent weight lost relative to starting weight using two independent experiments with 6 mice/group; results are listed in Table 3). (C) We completed ELISAs to quantify total H1-reactive Abs in each of our pooled serum samples and found that there were different amounts of HA Abs in each serum pool. (D) We repeated passive transfer studies after normalizing serum amounts so that equal amounts of HA Abs were transferred. Mice that received uninfected HAI^{high} or uninfected HAI^{low} pooled sera (gray and blue lines, respectively) were protected similarly against severe influenza disease, with mice that received uninfected HAI^{high} pooled sera recovering more quickly than mice that received uninfected HAI^{low} pooled sera (results are given with ±SEM; 1-way ANOVA was performed for each day postinfection based on percent weight lost relative to starting weight using one independent experiment with 6 mice/group; results are listed in Table 4).

increase in titer). In our study, HAI titers were independently associated with protection in adjusted models; however, HA stalk Abs were not. However, the effects of both HAI and HA stalk Ab titers were only slightly attenuated in our adjusted model, and it is possible that our relatively small sample size limited our ability to detect an independent association between HA stalk titers and protection.

There are several limitations to our study. Since our sample size was relatively small, we only evaluated the contribution of Abs to the HA head and stalk. Larger studies will be required to independently evaluate other immune correlates of protection. For example, it will be important for future studies to evaluate the relationship between HA head and stalk Ab-associated protection and neuraminidase (NA) Ab-associated pro-

TABLE 3 One-way ANOVA results for passive transfer normalized by volume[a]

Comparison	Result by dpi														
	1	2	3	4	5	6	7	8	9	10	11	12	13	14	15
PBS vs uninfected HAI^{high}	0.9535, NS	0.8290, NS	0.2205, NS	0.0133*	0.0004*	<0.0001****	<0.0001****	<0.0001****	<0.0001****	<0.0001****	<0.0001****	<0.0001****	0.0004***	0.0048**	0.0175*
PBS vs uninfected HAI^{low}	0.7722, NS	0.6513, NS	0.1259, NS	0.0222*	0.0013**	0.0017**	0.0017**	0.0094**	0.0070**	0.0028**	0.0062**	0.0688, NS	0.0757, NS	0.2567, NS	0.3884, NS
PBS vs infected HAI^{low}	0.9840, NS	0.9535, NS	0.5620, NS	0.8066, NS	0.4905, NS	0.2181, NS	0.5920, NS	0.0775, NS	0.0543, NS	0.0356*	0.0150*	0.0570, NS	0.1593, NS	0.4164, NS	0.5456, NS
Uninfected HAI^{high} vs uninfected HAI^{low}	0.7604, NS	0.9938, NS	0.9967, NS	0.9897, NS	0.9466, NS	0.1707, NS	0.0020***	0.0001***	0.0008***	0.0069**	0.0709, NS	0.0480*	0.1517, NS	0.2574, NS	0.3808, NS
Uninfected HAI^{high} vs infected HAI^{low}	0.9728, NS	0.9839, NS	0.8833	0.1011, NS	0.0173*	0.0012**	<0.0001****	<0.0001****	<0.0001****	0.0003***	0.0228*	0.0422*	0.0558, NS	0.1218, NS	0.2207, NS
Uninfected HAI^{low} vs infected HAI^{low}	0.9312, NS	0.9155, NS	0.7605, NS	0.1609, NS	0.0512, NS	0.1735, NS	0.4706, NS	0.7751, NS	0.7989, NS	0.6871, NS	0.9693, NS	>0.9999, NS	0.9690, NS	0.9809, NS	0.9886, NS

[a]One-way ANOVA with Tukey's correction for multiple comparisons performed for each day postinfection. The P value for each comparison is reported, calculated on the percent weight lost compared to the baseline for each group each day. Data in this table are depicted in Fig. 5B. NS, not significant. *, $P \leq 0.05$; **, $P \leq 0.01$; ***, $P \leq 0.001$; ****, $P \leq 0.0001$.

TABLE 4 One-way ANOVA results for passive transfer normalized by HA titer[a]

Comparison	Result by dpi														
	1	2	3	4	5	6	7	8	9	10	11	12	13	14	15
PBS vs uninfected HAI^{high}	0.7715, NS	0.1346, NS	0.5014, NS	0.1318, NS	0.0005***	<0.0001****	<0.0001****	<0.0001****	<0.0001****	<0.0001****	<0.0001****	<0.0001****	<0.0001****	<0.0001****	<0.0001****
PBS vs uninfected HAI^{low}	0.4401, NS	0.9592, NS	0.8084, NS	0.3562, NS	0.0851, NS	0.0034**	<0.0001****	<0.0001****	<0.0001****	<0.0001****	<0.0001****	<0.0001****	<0.0001****	<0.0001****	<0.0001****
PBS vs infected HAI^{low}	0.0727, NS	0.2528, NS	0.7643, NS	0.3626, NS	0.4106, NS	0.8007, NS	0.7025, NS	0.0039**	0.0001***	<0.0001****	<0.0001****	<0.0001****	<0.0001****	0.0001***	0.0004***
Uninfected HAI^{high} vs uninfected HAI^{low}	0.9413, NS	0.0516, NS	0.9513, NS	0.9271, NS	0.1217, NS	0.1124, NS	0.0920, NS	0.0210*	0.0283*	0.0335*	0.1813, NS	0.0442*	0.1948, NS	0.5458, NS	0.5089, NS
Uninfected HAI^{high} vs infected HAI^{low}	0.3752, NS	0.0023**	0.1100, NS	0.0038**	<0.0001****	<0.0001****	<0.0001****	<0.0001****	<0.0001****	<0.0001****	0.0005***	<0.0001****	0.0023**	0.0047**	0.0225, NS
Uninfected HAI^{low} vs infected HAI^{low}	0.7028, NS	0.5014, NS	0.2722, NS	0.0151*	0.0028**	0.0004***	<0.0001****	0.0011**	0.0051**	0.0111*	0.0573, NS	0.0353*	0.1734, NS	0.0803, NS	0.3097, NS

[a]One-way ANOVA with Tukey's correction for multiple comparisons performed for each day postinfection. The P value for each comparison is reported, calculated on the percent weight lost compared to the baseline for each group each day. Data in this table are depicted in Fig. 5D. NS, not significant. *, $P \leq 0.05$; **, $P \leq 0.01$; ***, $P \leq 0.001$; ****, $P \leq 0.0001$.

tection. Recent studies have shown that NA Abs are associated with protection in an H1N1 challenge cohort (36), and NA Abs were also identified as an independent correlate of protection in a controlled vaccine efficacy study (64). It will be critical to determine if NA Ab-associated protection is independent of the protective effects of HA head and stalk Abs.

It should be noted that participants in our study were likely admitted to the hospital at various days postinfection. While most blood specimens were collected relatively early (≤3 days after symptom onset), we cannot exclude that some participants in our studies were infected for a prolonged period of time before being admitted to the hospital. This raises the possibility that some participants have already mounted *de novo* Ab responses to H1N1 infection, which could convolute the analyses of Ab types associated with protection. While this is a possibility, it is less of a concern since we found that all infected individuals have very low HAI titers. If our infected participants were making *de novo* Ab responses, we would anticipate that some of them would have high HAI titers to the infecting H1N1 virus. In addition, Ab titers do not typically increase as days from symptom onset to blood specimen collection increases (42), which suggests that samples used in this study were collected prior to the generation of *de novo* Ab responses against the infecting virus.

It is interesting that *in vitro* neutralization titers (Fig. 4A), but not ADCC titers (Fig. 4D), were associated with H1N1 protection. *In vitro* neutralization activity is mainly driven by HA head Abs (5–9), whereas HA stalk Abs are more effective at ADCC (49). It should be noted that HA stalk IgG1 and IgA Abs have been shown to mediate phagocytosis with innate cellular partners (65), which could prove to be an important mechanism of protection by HA stalk Abs and should be considered in future studies. HA head Abs were associated with greater protection in our cohorts than stalk Abs (Table 2), and these Abs conferred protection superior to that of HA stalk Abs when passively transferred into mice (Fig. 4B and D). Interestingly, serum from HAI^{low} uninfected participants protected mice better than serum from HAI^{low} infected participants in passive transfer studies after normalizing total HA Ab amounts under each transfer condition. While these data suggest that HA stalk Abs can confer protection *in vivo*, we cannot rule out that other immune components (such as NA Abs) contributed to protection in these experiments.

Taken together, our findings provide important new insights into the prevalence and functionality of HA head and stalk Abs in humans. Future studies that tease out the interdependence of HA head and stalk Abs, as well as Abs and T cells against other viral antigens, will be useful in guiding the development of new universal influenza vaccine antigens.

MATERIALS AND METHODS

Human subjects. During the 2015–2016 influenza season, adult (≥18 years) patients hospitalized for treatment of acute respiratory illnesses at the University of Michigan Hospital in Ann Arbor, MI, and Henry Ford Hospital in Detroit, MI, were prospectively enrolled in a case test-negative design study of influenza vaccine effectiveness. All participants provided informed consent and were enrolled ≤10 days from illness onset during the period of influenza circulation (January to April of 2015 and 2016). Participants completed an enrollment interview and had throat and nasal swab specimens collected and combined for influenza virus identification. Influenza vaccination status was defined by self-report and documentation in the electronic medical record and Michigan Care Improvement Registry (MCIR). When available, clinical serum specimens collected as early as possible after hospital admission were retrieved; all specimens were collected ≤10 days from illness onset based on the enrollment case definition. Studies involving humans were approved by the Institutional Review Boards of the University of Michigan and University of Pennsylvania. All experiments (HAI, ELISAs, *in vitro* neutralization assays, ADCC assays, and passive transfers) were completed at the University of Pennsylvania using deidentified sera.

Viruses. Viruses possessing A/California/07/2009 HA and NA or A/HUP/04/2016 HA and NA were generated by reverse genetics using internal genes from A/Puerto Rico/08/1934. Viruses were engineered to possess the Q226R HA mutation, which facilitates viral growth in chicken eggs. Viruses were grown in fertilized chicken eggs, and the HA gene was sequenced to verify that additional mutations did not arise during propagation. We isolated the A/HUP/04/2016 virus from respiratory secretions obtained from a patient at the Hospital of the University of Pennsylvania in 2016. For this process, deidentified clinical material from the Hospital of the University of Pennsylvania Clinical Virology Laboratory was added to Madin-Darby canine kidney (MDCK) cells (originally obtained from the National Institutes of

Health) in serum-free medium with L-(tosylamido-2-phenyl) ethyl chloromethyl ketone (TPCK)-treated trypsin, HEPES, and gentamicin. Virus was isolated from the infected MDCK cells 3 days later. We extracted viral RNA and sequenced the HA gene of A/HUP/04/16.

Recombinant HA proteins. Plasmids encoding the recombinant headless HA stalk were provided by Adrian McDermott and Barney Graham from the Vaccine Research Center at the National Institutes of Health. The headless HA stalk protein was expressed in 293F cells and purified using nickel-nitrilotriacetic acid agarose (no. 1018244; Qiagen) in 5-ml polypropylene columns (no. 34964; Qiagen), washed with pH 8 buffer containing 50 mM Na_2HCO_3, 300 mM NaCl, and 20 mM imidazole, and then eluted using pH 8 buffer containing 50 mM Na_2HCO_3, 300 mM NaCl, and 300 mM imidazole. Purified protein was buffer exchanged into phosphate-buffered saline (PBS; no. 21-031-CM; Corning). Following purification, the headless HA stalk proteins were biotinylated using the Avidity BirA-500 kit (no. BirA500) and stored in aliquots at −80°C. Plasmids encoding the recombinant chimeric (c6/H1) HA were provided by Florian Krammer (Mt. Sinai). The detailed protocol for expression of this protein is published elsewhere (46). In brief, the c6/H1 HA protein was expressed in High Five baculovirus cells and purified using the same methods referenced for the headless HA stalk protein. Purified protein was buffer exchanged into PBS (no. 21-031-CM; Corning) and stored in aliquots at −80°C.

MAbs. Plasmids encoding the human MAb EM-4C04, 70-1F02, and CR9114 IgG1 isotypes were provided by Patrick Wilson at the University of Chicago. The heavy-chain constant regions for IgG2, IgG3, and IgA (sequences listed below) were synthesized as a gBlock by IDT and cloned into the pSport6 vector containing the heavy chain of CR9114. All MAbs were expressed in 293T cells and purified 4 days postinfection using NAb protein A/G spin kits (no. 89950; Thermo Fisher) for the IgG isotypes or using peptide M agarose (no. gel-pdm-2; InvivoGen) for the IgA isotype.

The IgG2 sequence is CGCATGATGCGTCGACCAAGGGTCCTAGCGTTTTCCCGCTCGCACCTTGTAGTCGG
AGCACCTCCGAATCTACGGCGGCGCTCGGATGTCTGGTTAAGGATTACTTTCCTGAACCTGTTACTGTATCTTGG
AATTCAGGAGCACTGACATCTGGTGTACATACTTTTCCAGCGGTTTTGCAGTCATCTGGTCTTTATTCCCTGTCCA
GTGTGGTAACAGTACCATCCTCAAACTTTGGAACTCAGACCTATACCTGCAATGTGGACCACAAGCCATCCAATA
CAAAAGTCGATAAGACTGTCGAGCGGAAGTGCTGTGTCGAATGCCCTCCCTGCCCCGCTCCGCCGGTTGCAGGG
CCAAGTGTATTTCTTTTTCCACCAAAACCAAAAGATACGCTTATGATATCTCGCACGCCTGAAGTAACCTGCGTAG
TCGTTGATGTAAGTCACGAGGATCCCGAAGTTCAATTCAATTGGTATGTAGATGGCGTTGAAGTGCATAATGCAA
AGACCAAACCTAGAGAAGAACAATTCAATAGTACCTTTCGCGTGGTTAGCGTACTCACAGTCGTCCACCAGGATT
GGCTGAATGGGAAGGAGTACAAATGCAAGGTCTCTAACAAAGGTCTTCCGGCCCCCATAGAAAAAACGATCAG
TAAGACCAAGGGGCAGCCCAGAGAGCCACAGGTTTATACGTTGCCTCCGTCTCGCGAGGAAATGACTAAAAAC
CAGGTCAGCCTGACTTGTTTGGTGAAAGGGTTTTACCCGAGCGATATTGCTGTGGAATGGGAGAGTAACGGGCA
ACCGGAGAACAATTACAAAACGACACCGCCCATGCTTGATAGTGATGGTTCCTTCTTCTTGTACAGCAAGTTGAC
GGTTGATAAATCCAGGTGGCAGCAAGGAAATGTTTTCTCTTGTTCAGTGATGCATGAGGCGCTCCACAACCATTA
TACGCAAAAATCACTCTCACTTTCACCGGGGAAATGAAGCTTGAGCAGGGCCT.

The IgG3 sequence is CGCATGATGCGTCGACCAAAGGGCCGTCAGTCTTTCCCTTGGCGCCGTGCTCCAGG
AGTACCAGCGGCGGCACCGCGGCGTTGGGATGTCTTGTCAAGGATTATTTTCCCGAACCCGTCACCGTAAGCTG
GAACAGTGGGGCATTGACGTCTGGCGTTCATACTTTTCCGGCAGTACTTCAGAGTTCCGGCCTTTATTCTTTGTCA
AGCGTTGTTACCGTACCATCCAGTAGCCTTGGCACCCAGACCTACACCTGTAATGTTAATCACAAACCAAGTAAC
ACCAAGGTTGATAAGAGGGTTGAGCTTAAAACACCGCTTGGTGACACAACCCATACGTGTCCAAGATGTCCGGA
GCCGAAGAGTTGTGATACCCCGCCGCCGTGTCCTCGCTGTCCGGAACCAAAGAGCTGTGATACCCCCCCACCTT
GTCCCAGATGTCCTGAACCGAAATCATGTGACACGCCACCACCTTGCCCAAGATGTCCCGCGCCAGAGCTGCTG
GGTGGGCCCAGCGTATTTCTTTTTCCACCCAAACCGAAGGATACCCTTATGATAAGCAGGACTCCCGAGGTTACC
TGCGTGGTGGTTGACGTAAGTCACGAAGACCCCGAAGTCCAATTCAAATGGTATGTTGATGGGGTCGAAGTACA
CAACGCGAAGACTAAACCGAGAGAGGAACAGTATAATAGCACATTCCGGGTTGTTTCCGTACTTACAGTACTTC
ATCAGGACTGGCTTAATGGCAAGGAGTACAAGTGCAAAGTCAGTAACAAGGCACTCCCTGCTCCGATTGAAAAG
ACAATATCAAAGACGAAAGGTCAACCCAGAGAGCCGCAGGTCTACACACTCCCTCCGTCCAGAGAAGAGATGA
CGAAAAACCAAGTTTCATTGACGTGCCTCGTTAAAGGATTCTACCCAAGCGACATAGCTGTTGAGTGGGAGAGC
AGCGGCCAGCCTGAGAACAATTATAATACTACCCCCCCCATGCTCGACTCTGATGGTAGTTTTTTTCTGTACTCCA
AGCTGACGGTAGACAAAAGTAGATGGCAGCAAGGCAACATCTTCAGTTGCTCTGTTATGCACGAGGCGTTGCAC
AACCGATTCACACAGAAGTCACTGAGCCTGTCTCCGGGTAAATGAAGCTTGAGCAGGGCCT.

The IgA sequence is CGCATGATGCGTCGACTTCTCCAAAAGTGTTTCCCCTCAGTTTGTGTTCCACTCAACC
GGATGGTAACGTGGTGATTGCTTGTCTCGTGCAAGGTTTTTTCCCACAGGAACCGCTGAGTGTTACATGGTCAGA
GTCAGGCCAAGGTGTAACCGCGCGCAACTTTCCCCCTTCACAGGACGCTAGTGGCGATCTGTATACTACCTCCTC
TCAGCTCACTCTTCCCGCCACACAATGCCTCGCTGGGAAATCTGTAACCTGCCACGTTAAACATTACACTAATCC
ATCACAGGACGTTACCGTGCCGTGCCCTGTACCATCCACGCCGCCTACGCCGTCACCGTCAACTCCTCCTACTCC
CTCACCCTCTTGTTGTCACCCGCGCCTCTCTCTTCACAGACCGGCCTTGGAGGACCTTCTCCTTGGGTCTGAGGCG
AATTTGACTTGCACGCTCACGGGGTTGCGGGACGCTAGTGGGGTTACGTTTACATGGACACCTTCATCAGGGAA
GTCTGCCGTTCAGGGCCCCCCAGAGCGCGATTTGTGCGGGTGTTACAGCGTATCTTCTGTGCTGCCTGGGTGCGC
TGAGCCCTGGAATCACGGCAAAACGTTTACCTGCACCGCTGCTTACCCAGAGAGCAAAACCCCTCTGACGGCTA
CATTGTCCAAGTCAGGCAACACATTTCGCCCCGAAGTCCACCTCTTGCCACCTCCATCCGAAGAACTCGCCCTGA
ACGAACTCGTGACGCTGACGTGCCTTGCACGCGGCTTTTCCCCGAAAGACGTTCTCGTCCGGTGGCTTCAAGGTT
CTCAGGAACTCCCACGGGAGAAGTACCTGACCTGGGCTTCACGCCAGGAACCTTCACAAGGGACGACCACTTTC
GCAGTCACGTCAATTCTGAGAGTTGCCGCTGAGGACTGGAAGAAGGGAGATACTTTCAGTTGTATGGTAGGTCA
CGAAGCACTGCCGCTGGCATTTACGCAGAAAACCATCGATCGGCTTGCCGGAAAGCCTACTCATGTTAACGTTTC
CGTAGTGATGGCGGAGGTAGATGGCACATGTTACTGAAGCTTGAGCAGGGCCT.

HAI assays. Serum samples were pretreated with receptor-destroying enzyme (no. 370013; Denka Seiken) followed by hemadsorption, in accordance with WHO recommended protocols (66). HAI titrations were performed in 96-well U-bottom plates (no. 353077; Corning). Sera were initially diluted 2-fold and

then added to four agglutinating doses of virus, for a final volume of 100 μl/well. Turkey erythrocytes (no. 7209401; Lampire) were added to each well (12.5 μl diluted to 2%, vol/vol). The erythrocytes were gently mixed with sera and virus and then allowed to incubate for 1 h at room temperature. Agglutination was read and HAI titers were expressed as the inverse of the highest dilution that inhibited four agglutinating doses of virus. Each HAI assay was performed independently on two different days.

Headless HA ELISAs. Headless HA ELISAs were performed on 96-well Immulon 4HBX flat-bottom microtiter plates (no. 3855; Thermo Fisher) coated with 0.5 μg/well of streptavidin (no. S4762; Sigma). We completed total IgG headless HA ELISAs with all serum samples and isotype headless HA ELISAs with serum samples that had sufficient volumes. Biotinylated headless HA protein was diluted in biotinylation buffer containing 1× Tris-buffered saline (TBS; no. 170-6435; Bio Rad), 0.005% Tween (no. 170-6531; Bio Rad), and 0.1% bovine serum albumin (no. A8022; Sigma) to 0.25 μg/ml, and 50 μl was added per well and incubated on a rocker for 1 h at room temperature. Each well was then blocked for an additional 1 h at room temperature using biotinylation blocking buffer containing 1× TBS (no. 170-6435; Bio Rad), 0.005% Tween 20 (no. 170-6531; Bio Rad), and 1% bovine serum albumin (no. A8022; Sigma). Each serum sample was serially diluted in biotinylation buffer (starting at 1:100 dilution for total IgG or 1:50 dilution for Ab isotype), added to the ELISA plates, and allowed to incubate for 1 h at room temperature on a rocker. As a control, we added the human CR9114 stalk-specific MAb, starting at 0.03 μg/ml, to verify equal coating of plates and to determine relative serum titers. Peroxidase-conjugated goat anti-human IgG (no. 109-036-098; Jackson), peroxidase-conjugated mouse anti-human IgG1 (no. 9054-05; Southern Biotech), peroxidase-conjugated mouse anti-human IgG2 (no. 9060-05; Southern Biotech), peroxidase-conjugated mouse anti-human IgG3 (no. 9210-05; Southern Biotech), or peroxidase-conjugated goat anti-human IgA (no. 2050-05; Southern Biotech) was incubated for 1 h at room temperature on a rocker. Finally, SureBlue TMB peroxidase substrate (no. 5120-0077; KPL) was added to each well, and the reaction was stopped with the addition of 250 mM HCl solution. Plates were extensively washed with PBS (no. 21-031-CM; Corning) and 0.1% Tween 20 (no. 170-6531; Bio Rad) between each step using a BioTek 405 LS microplate washer. Relative titers were determined using a consistent concentration of the CR9114 MAb for each plate and reported as the corresponding inverse of the serum dilution that generated the equivalent optical densities (OD). Each type of ELISA (total IgG, IgG1, IgG2, IgG3, and IgA) was performed twice.

Chimeric (c6/H1) HA ELISAs. Chimeric HA ELISAs were performed on 96-well Immulon 4HBX flat-bottom microtiter plates (no. 3855; Thermo Fisher). HA proteins were diluted in PBS (no. 21-031-CM; Corning) to 2 μg/ml and coated at 50 μl per well overnight at 4°C. Plates were blocked using an ELISA buffer containing 3% goat serum (no. 16210-064; Gibco), 0.5% milk (no. DSM17200-1000; Dot Scientific, Inc.), and 0.1% Tween 20 (no. 170-6531; Bio Rad) in PBS (no. 21-031-CM; Corning) 1× for 2 h at room temperature. Each serum sample was serially diluted in the ELISA buffer (starting at 1:100 dilutions), added to the ELISA plates, and allowed to incubate for 2 h at room temperature. As a control, we added the human CR9114 stalk-specific MAb, starting at 0.03 μg/ml, to verify equal coating of plates and to determine relative serum titers. Peroxidase-conjugated goat anti-human IgG (no. 109-036-098; Jackson) next was incubated for 1 h at room temperature. Finally, SureBlue TMB peroxidase substrate (no. 5120-0077; KPL) was added to each well, and the reaction was stopped with the addition of 250 mM HCl solution. Plates were extensively washed with PBS (no. 21-031-CM; Corning) and 0.1% Tween 20 (no. 170-6531; Bio Rad) between each step using a BioTek 405 LS microplate washer. Relative titers were determined using a consistent concentration of the CR9114 MAb for each plate and reported as the corresponding inverse of the serum dilution that generated the equivalent OD. Each ELISA was performed twice.

Competition ELISAs. Competition ELISAs were performed on 96-well Immulon 4HBX flat-bottom microtiter plates (no. 3855; Thermo Fisher). HA proteins were diluted in 1× Dulbecco's PBS (DPBS; no. 21-031-CM; Corning) to 2 μg/ml and coated at 50 μl per well overnight at 4°C. Plates were blocked using the biotinylation blocking buffer, described earlier, for 2 h at room temperature. Each serum sample was serially diluted in biotinylation buffer (starting at 1:10 dilution), added to the ELISA plates, and allowed to incubate for 1 h at room temperature before adding human 70-1F02 MAb (specific for the conformationally dependent HA stalk epitope 1 [67]) that had been biotinylated using the Invitrogen SiteClick biotin antibody labeling kit (no. S20033; Thermo Fisher) at a constant concentration of 0.03 μg/ml and incubated at room temperature for an additional hour. As a control, we added the human CR9114 stalk-specific MAb, starting at 0.03 μg/ml, to verify equal coating of plates and to determine relative serum titers. Peroxidase-conjugated streptavidin (no. 554066; BD Pharmingen) next was incubated for 1 h at room temperature. Finally, SureBlue TMB peroxidase substrate (no. 5120-0077; KPL) was added to each well, and the reaction was stopped with the addition of 250 mM HCl solution. Plates were extensively washed with PBS (no. 21-031-CM; Corning) and 0.1% Tween 20 (no. 170-6531; Bio Rad) between each step, with the exception of the addition of biotinylated 70-1F02, using a BioTek 405 LS microplate washer. Relative titers were determined using the uncompeted control lane OD (biotinylated 70-1F02 binding in the absence of sera) and setting that OD to 100%. Each serum sample was then assessed by nonlinear regression using GraphPad Prism. Titers are reported as the inverse of the highest serum dilution that inhibited binding of the biotinylated 70-1F02 to 30% of the uncompeted binding. Each competition ELISA was performed independently on two different days.

***In vitro* neutralization assays.** *In vitro* neutralization assays were completed using a subset of samples. We excluded samples that had limited amounts of sera. Plasmids encoding pH1N1 viruses possessing genes encoding eGFP in place of most of the PB1 gene segment were provided by Jesse Bloom at The Fred Hutchinson Cancer Research Center. The eGFP segment retained the noncoding and 80 terminal coding nucleotides, allowing this segment to be efficiently and stably packaged into the

virions. Detailed protocols for the reverse genetics, expression, and *in vitro* neutralization assays using the recombinant viruses have been published elsewhere (61, 68). In brief, serum was pretreated with receptor-destroying enzyme (no. 370013; Denka Seiken) and then serially diluted in neutralization assay medium (Medium 199; no. 11150-059; Gibco) supplemented with 0.01% heat-inactivated fetal bovine serum (FBS; no. F0926-100; Sigma), 0.3% bovine serum albumin (no. A8022; Sigma), 100 U penicillin–100 μg streptomycin/ml (no. 30-002-Cl; Corning), 100 μg of calcium chloride/ml (no. S7653; Sigma), and 25 mM HEPES (no. 25-060-Cl; Corning), beginning at a 1:80 dilution. PB1flank-eGFP viruses were then added to the serum dilutions and were incubated at 37°C for 1 h to allow for neutralization. As a control, the human CR9114 HA stalk-specific MAb was added to ensure equal infectivity and neutralization across all plates. Viruses and sera then were transferred to 96-well flat-bottom tissue culture plates containing 80,000 cells per well of MDCK-SIAT1-TMPRSS2 cells constitutively expressing PB1 under a cytomegalovirus promoter. Plates were incubated at 37°C for 30 h postinfection. Mean fluorescent intensity of samples was read using an Envision plate reader (monochromator, top read, excitation filter at 485 nm, emission filter at 530 nm). Neutralization titers were reported as the inverse of the highest dilution that decreased mean fluorescence by 90% relative to infected control wells in the absence of antibodies. Each neutralization assay was performed independently on two different days.

ADCC activity assays. ADCC activity assays were completed using a subset of samples. We excluded samples that had limited amounts of sera. 293T cells were plated at 3.5e4 cells per well in a 96-well flat-bottom tissue culture plate (no. 353072; Corning) 24 h before transfection. 293T cells were then transfected using 20 μl Opti-MEM (no. 31985-070; Gibco), 1 μl Lipofectamine 2000 (no. 11668-019; Invitrogen), and 500 ng plasmids encoding the HA gene from A/California/07/09 per well and incubated at 37°C for approximately 30 h before performing the ADCC assay. Approximately 12 h before performing the ADCC assay, frozen PBMCs from four separate donors (obtained through the University of Pennsylvania Human Immunology Core) were thawed at 37°C and then washed 3× using 15 ml of warmed complete RPMI medium (no. 10-040-CM; Corning) (supplemented with 10% heat-inactivated FBS [no. F0926-100; Sigma], 1% penicillin-streptomycin [no. 30-002-Cl; Corning]). Each aliquot of PBMCs was then transferred to a 50-ml conical tube and rested overnight in 23 ml of complete RPMI medium at a 5° angle, with the cap loosened to allow for gas exchange. On the day of the assay, serum samples were diluted in Dulbecco's modified Eagle's medium (no. 10-013-CM; Corning) supplemented with 10% FBS (no. F0926-100; Sigma) at a 1:10 dilution. As a control for this assay, the human CR9114 HA stalk-specific MAb was included at a concentration of 5 μg/ml to ensure efficient activation of ADCC. Transfected 293T cells were loosened by pipetting and transferred to a 96-well U-bottom plate (no. 353077; Corning) and spun down for 1 min at 1,200 rpm, and the medium was flicked out. The serum/MAb dilutions were transferred to the plates containing the transfected 293T cells and were mixed with the transfected cells by gentle pipetting and incubated at 37°C for 2 h. PBMC aliquots were combined, spun down, and counted, and a master mix of 2e7 cells/ml was set up using complete RPMI medium. Aliquots of the PBMC master mix were set up for the live/dead and unstained control wells. Phycoerythrin-conjugated mouse anti-human CD107a (no. 328608; BioLegend) was added at a 1:50 dilution. Brefeldin A (no. B7651; Sigma) was added to 10 μg/ml. Monensin (no. 51-2092KZ; BD BioSciences) was added to 5 μl per 1 ml of PBMC master mix concentration. An aliquot of 200 μl was made, phorbol myristate acetate (no. P1585; Sigma) was added to a 5 μg/ml concentration, and ionomycin (no. I9657; Sigma) was added to a 1 μg/ml concentration. Serum/cell suspensions were spun down at 1,200 rpm for 1 min, and medium was flicked out. The PBMC master mix and the aliquots for the various controls were plated at 50 μl per well and mixed gently by pipetting, followed by incubation at 37°C for 4 h. Cells were then stained in the following manner. Live/dead fixable near-infrared stain (no. L34976; Thermo) was diluted 1:50 in DPBS (no. 21-031-CM; Corning) and 1% bovine serum albumin (no. A8022; Sigma) for 30 min in the dark at 4°C. Human FcR blocking reagent (no. 130-059-901; Miltenyi Biotec) was diluted 1:25 in DPBS (no. 21-031-CM; Corning) and 1% bovine serum albumin (no. A8022; Sigma) and incubated in the dark for 10 min at 4°C. Alexa Fluor 647-conjugated mouse anti-human-CD3 (no. 344826; BioLegend) and BV421-conjugated mouse anti-human CD56 (no. 318328; BioLegend) were diluted 1:200 in DPBS (no. 21-031-CM; Corning) plus 1% bovine serum albumin (no. A8022; Sigma) and incubated in the dark for 30 min at room temperature. Cells were then fixed using 10% paraformaldehyde (no. 15714-S; Electron Microscopy Sciences) diluted in MilliQ water for 6 min at room temperature. Cells were extensively washed with DPBS (no. 21-031-CM; Corning) and 1% bovine serum albumin (no. A8022; Sigma) between each step. Cells were stored overnight at 4°C in 100 μl/well of DPBS (no. 21-031-CM; Corning) and 1% bovine serum albumin (no. A8022; Sigma). Flow cytometry was performed using and LSRII (BD Biosciences, San Diego, CA). Compensation controls were set up using anti-mouse Igκ beads (no. 552843; BD BioSciences) and run for each antibody for every experiment, and voltages were adjusted accordingly. All data were analyzed in FlowJo (Ashland, OR) by gating on single cells that were $CD3^-$ $CD56^+$ $CD107a^+$ in control wells that did not contain serum/MAb to adjust for basal levels of CD107a expression. These gates were then applied to each serum sample, and ADCC activity was expressed as a percentage of NK cells expressing $CD107a^+$. Each ADCC assay was performed independently on three different days, and the same four PBMC donors were pooled and used for each replicate.

Murine experiments. All mouse experiments were reviewed and approved by the IACUCs of the Wistar Institute and University of Pennsylvania. All passive transfer experiments were performed in humanized FcR mice (hFcgR [1, 2a, 2 b, 3a, 3b]tg^+/mFcgR alpha chain [1, 2 b, 3, 4]$^{-/-}$) that were provided by Jeffrey Ravetch at the Rockefeller University (63). Sera were pooled into three groups, uninfected HAI^{high} (>40 HAI titer), uninfected HAI^{low} (≤ 40 HAI titer), and infected HAI^{low} (≤ 40 HAI titer), and then heat treated for 30 min at 55°C. Serum or sterile PBS was then transferred into mice by intraperitoneal injection. Four hours posttransfer, mice were bled by submandibular puncture, anesthetized using

isoflurane, and challenged intranasally using 50 μl of sterile PBS containing a sublethal dose (9e4 50% tissue culture infective dose units) of A/California/07/09. ELISAs were run on the sera collected from each animal to verify that the passive transfer was successful. Mice were weighed on the day on infection and then daily for 15 days postinfection. Weight loss was reported as percent weight loss relative to the starting weight of each mouse. For the passive transfer normalized by volume, two independent experiments were performed using a mix of male and female humanized FcR mice for a total of 6 mice per group per experiment. For the passive transfer normalized by HA antibody titer, a single experiment was performed using a mix of male and female humanized FcR mice for a total of 6 mice per group, since we had limited amounts of sera available for this study. One-way analysis of variance (ANOVA) was performed for each day postinfection between groups using GraphPad Prism software.

Statistical analysis. Fisher's exact tests, one-way ANOVAs, and Welch's *t* tests were completed using GraphPad software. Both unadjusted and adjusted logistic regression analyses were performed using R Studio (version 1.0.153).

ACKNOWLEDGMENTS

This work was supported by the National Institute of Allergy and Infectious Diseases (1R01AI113047, S.E.H.; 1R01AI108686, S.E.H.; 1R01AI097150, A.S.M.; CEIRS HHSN272201400005C, S.E.H. and A.S.M.; TL1TR001880, S.R.C.) and the Centers for Disease Control and Prevention (U01IP000474, A.S.M.). S.E.H. holds an Investigators in the Pathogenesis of Infectious Disease Award from the Burroughs Wellcome Fund.

We thank Florian Krammer (Mt. Sinai), Jesse Bloom (Fred Hutchinson Cancer Center), Patrick Wilson (University of Chicago), Barney Graham (Vaccine Research Center, NIH), and Adrian McDermott (Vaccine Research Center, NIH) for providing plasmids for this study. We thank Jeffrey Ravetch (Rockefeller University) for providing breeding pairs of humanized FcR mice.

A.S.M. has received consultancy fees from Sanofi Pasteur, Seqirus, and Novavax for work unrelated to this report. S.E.H. has received consultancy fees from Sanofi Pasteur, Lumen, Novavax, and Merck for work unrelated to this report. All other authors have no potential conflicts to declare.

REFERENCES

1. Pebody RG, Warburton F, Ellis J, Andrews N, Thompson C, von Wissmann B, Green HK, Cottrell S, Johnston J, de, Lusignan S, Moore C, Gunson R, Robertson C, McMenamin J, Zambon M. 2015. Low effectiveness of seasonal influenza vaccine in preventing laboratory-confirmed influenza in primary care in the United Kingdom: 2014/15 mid-season results. Euro Surveill 20:21025.
2. Skowronski DM, Chambers C, Sabaiduc S, De Serres G, Dickinson JA, Winter AL, Drews SJ, Fonseca K, Charest H, Gubbay JB, Petric M, Krajden M, Kwindt TL, Martineau C, Eshaghi A, Bastien N, Li Y. 2015. Interim estimates of 2014/15 vaccine effectiveness against influenza A(H3N2) from Canada's Physician Surveillance Network, January 2015. Euro Surveill 29:21022.
3. Johnson NP, Mueller J. 2002. Updating the accounts: global mortality of the 1918-1920 "Spanish" influenza pandemic. Bull Hist Med 76:105–115. https://doi.org/10.1353/bhm.2002.0022.
4. Webster RG, Braciale TJ, Monto AS, Lamb RA. 2013. Textbook of influenza, 2nd ed. Wiley-Blackwell, Chichester, West Sussex, United Kingdom.
5. Victora GD, Wilson PC. 2015. Germinal center selection and the antibody response to influenza. Cell 163:545–548. https://doi.org/10.1016/j.cell.2015.10.004.
6. Caton AJ, Brownlee GG, Yewdell JW, Gerhard W. 1982. The antigenic structure of the influenza virus A/PR/8/34 hemagglutinin (H1 subtype). Cell 31:417–427. https://doi.org/10.1016/0092-8674(82)90135-0.
7. Gerhard W, Yewdell J, Frankel ME, Webster R. 1981. Antigenic structure of influenza virus haemagglutinin defined by hybridoma antibodies. Nature 290:713–717. https://doi.org/10.1038/290713a0.
8. Angeletti D, Gibbs JS, Angel M, Kosik I, Hickman HD, Frank GM, Das SR, Wheatley AK, Prabhakaran M, Leggat DJ, McDermott AB, Yewdell JW. 2017. Defining B cell immunodominance to viruses. Nat Immunol 18:456–463. https://doi.org/10.1038/ni.3680.
9. Altman MO, Bennink JR, Yewdell JW, Herrin BR. 2015. Lamprey VLRB response to influenza virus supports universal rules of immunogenicity and antigenicity. Elife 4:e07467. https://doi.org/10.7554/eLife.07467.
10. Krammer F, Palese P. 2013. Influenza virus hemagglutinin stalk-based antibodies and vaccines. Curr Opin Virol 3:521–530. https://doi.org/10.1016/j.coviro.2013.07.007.
11. Brandenburg B, Koudstaal W, Goudsmit J, Klaren V, Tang C, Bujny MV, Korse HJ, Kwaks T, Otterstrom JJ, Juraszek J, van Oijen AM, Vogels R, Friesen RH. 2013. Mechanisms of hemagglutinin targeted influenza virus neutralization. PLoS One 8:e80034. https://doi.org/10.1371/journal.pone.0080034.
12. Tan GS, Lee PS, Hoffman RM, Mazel-Sanchez B, Krammer F, Leon PE, Ward AB, Wilson IA, Palese P. 2014. Characterization of a broadly neutralizing monoclonal antibody that targets the fusion domain of group 2 influenza A virus hemagglutinin. J Virol 88:13580–13592. https://doi.org/10.1128/JVI.02289-14.
13. Krammer F, Palese P. 2015. Advances in the development of influenza virus vaccines. Nat Rev Drug Discov 14:167–182. https://doi.org/10.1038/nrd4529.
14. Ekiert DC, Friesen RH, Bhabha G, Kwaks T, Jongeneelen M, Yu W, Ophorst C, Cox F, Korse HJ, Brandenburg B, Vogels R, Brakenhoff JP, Kompier R, Koldijk MH, Cornelissen LA, Poon LL, Peiris M, Koudstaal W, Wilson IA, Goudsmit J. 2011. A highly conserved neutralizing epitope on group 2 influenza A viruses. Science 333:843–850. https://doi.org/10.1126/science.1204839.
15. Corti D, Voss J, Gamblin SJ, Codoni G, Macagno A, Jarrossay D, Vachieri SG, Pinna D, Minola A, Vanzetta F, Silacci C, Fernandez-Rodriguez BM, Agatic G, Bianchi S, Giacchetto-Sasselli I, Calder L, Sallusto F, Collins P, Haire LF, Temperton N, Langedijk JP, Skehel JJ, Lanzavecchia A. 2011. A neutralizing antibody selected from plasma cells that binds to group 1 and group 2 influenza A hemagglutinins. Science 333:850–856. https://doi.org/10.1126/science.1205669.
16. Corti D, Suguitan AL, Jr, Pinna D, Silacci C, Fernandez-Rodriguez BM, Vanzetta F, Santos C, Luke CJ, Torres-Velez FJ, Temperton NJ, Weiss RA, Sallusto F, Subbarao K, Lanzavecchia A. 2010. Heterosubtypic neutralizing antibodies are produced by individuals immunized with a seasonal influenza vaccine. J Clin Investig 120:1663–1673. https://doi.org/10.1172/JCI41902.
17. Sui J, Hwang WC, Perez S, Wei G, Aird D, Chen LM, Santelli E, Stec B,

Cadwell G, Ali M, Wan H, Murakami A, Yammanuru A, Han T, Cox NJ, Bankston LA, Donis RO, Liddington RC, Marasco WA. 2009. Structural and functional bases for broad-spectrum neutralization of avian and human influenza A viruses. Nat Struct Mol Biol 16:265–273. https://doi.org/10.1038/nsmb.1566.
18. Margine I, Hai R, Albrecht RA, Obermoser G, Harrod AC, Banchereau J, Palucka K, Garcia-Sastre A, Palese P, Treanor JJ, Krammer F. 2013. H3N2 influenza virus infection induces broadly reactive hemagglutinin stalk antibodies in humans and mice. J Virol 87:4728–4737. https://doi.org/10.1128/JVI.03509-12.
19. Nachbagauer R, Krammer F. 2017. Universal influenza virus vaccines and therapeutic antibodies. Clin Microbiol Infect 23:222–228. https://doi.org/10.1016/j.cmi.2017.02.009.
20. Linderman SL, Chambers BS, Zost SJ, Parkhouse K, Li Y, Herrmann C, Ellebedy AH, Carter DM, Andrews SF, Zheng NY, Huang M, Huang Y, Strauss D, Shaz BH, Hodinka RL, Reyes-Teran G, Ross TM, Wilson PC, Ahmed R, Bloom JD, Hensley SE. 2014. Potential antigenic explanation for atypical H1N1 infections among middle-aged adults during the 2013-2014 influenza season. Proc Natl Acad Sci U S A 111:15798–15803. https://doi.org/10.1073/pnas.1409171111.
21. Zost SJ, Parkhouse K, Gumina ME, Kim K, Diaz Perez S, Wilson PC, Treanor JJ, Sant AJ, Cobey S, Hensley SE. 2017. Contemporary H3N2 influenza viruses have a glycosylation site that alters binding of antibodies elicited by egg-adapted vaccine strains. Proc Natl Acad Sci U S A 114:12578–12583. https://doi.org/10.1073/pnas.1712377114.
22. Paules CI, Marston HD, Eisinger RW, Baltimore D, Fauci AS. 2017. The pathway to a universal influenza vaccine. Immunity 47:599–603. https://doi.org/10.1016/j.immuni.2017.09.007.
23. Wrammert J, Koutsonanos D, Li GM, Edupuganti S, Sui J, Morrissey M, McCausland M, Skountzou I, Hornig M, Lipkin WI, Mehta A, Razavi B, Del Rio C, Zheng NY, Lee JH, Huang M, Ali Z, Kaur K, Andrews S, Amara RR, Wang Y, Das SR, O'Donnell CD, Yewdell JW, Subbarao K, Marasco WA, Mulligan MJ, Compans R, Ahmed R, Wilson PC. 2011. Broadly cross-reactive antibodies dominate the human B cell response against 2009 pandemic H1N1 influenza virus infection. J Exp Med 208:181–193. https://doi.org/10.1084/jem.20101352.
24. Yamayoshi S, Uraki R, Ito M, Kiso M, Nakatsu S, Yasuhara A, Oishi K, Sasaki T, Ikuta K, Kawaoka Y. 2017. A broadly reactive human anti-hemagglutinin stem monoclonal antibody that inhibits influenza A virus particle release. EBioMedicine 17:182–191. https://doi.org/10.1016/j.ebiom.2017.03.007.
25. Krammer F, Hai R, Yondola M, Tan GS, Leyva-Grado VH, Ryder AB, Miller MS, Rose JK, Palese P, García-Sastre A, Albrecht RA. 2014. Assessment of influenza virus hemagglutinin stalk-based immunity in ferrets. J Virol 88:3432–3442. https://doi.org/10.1128/JVI.03004-13.
26. Jacobsen H, Rajendran M, Choi A, Sjursen H, Brokstad KA, Cox RJ, Palese P, Krammer F, Nachbagauer R. 2017. Influenza virus hemagglutinin stalk-specific antibodies in human serum are a surrogate marker for in vivo protection in a serum transfer mouse challenge model. mBio 8:e01463-17. https://doi.org/10.1128/mBio.01463-17.
27. Baranovich T, Jones JC, Russier M, Vogel P, Szretter KJ, Sloan SE, Seiler P, Trevejo JM, Webby RJ, Govorkova EA. 2016. The hemagglutinin stem-binding monoclonal antibody VIS410 controls influenza virus-induced acute respiratory distress syndrome. Antimicrob Agents Chemother 60:2118–2131. https://doi.org/10.1128/AAC.02457-15.
28. Throsby M, van den Brink E, Jongeneelen M, Poon LL, Alard P, Cornelissen L, Bakker A, Cox F, van Deventer E, Guan Y, Cinatl J, ter Meulen J, Lasters I, Carsetti R, Peiris M, de Kruif J, Goudsmit J. 2008. Heterosubtypic neutralizing monoclonal antibodies cross-protective against H5N1 and H1N1 recovered from human IgM+ memory B cells. PLoS One 3:e3942. https://doi.org/10.1371/journal.pone.0003942.
29. Wang TT, Tan GS, Hai R, Pica N, Petersen E, Moran TM, Palese P. 2010. Broadly protective monoclonal antibodies against H3 influenza viruses following sequential immunization with different hemagglutinins. PLoS Pathog 6:e1000796. https://doi.org/10.1371/journal.ppat.1000796.
30. Yassine HM, Boyington JC, McTamney PM, Wei CJ, Kanekiyo M, Kong WP, Gallagher JR, Wang L, Zhang Y, Joyce MG, Lingwood D, Moin SM, Andersen H, Okuno Y, Rao SS, Harris AK, Kwong PD, Mascola JR, Nabel GJ, Graham BS. 2015. Hemagglutinin-stem nanoparticles generate heterosubtypic influenza protection. Nat Med 21:1065–1070. https://doi.org/10.1038/nm.3927.
31. Nachbagauer R, Krammer F, Albrecht RA. 2018. A live-attenuated prime, inactivated boost vaccination strategy with chimeric hemagglutinin-based universal influenza virus vaccines provides protection in ferrets: a confirmatory study. Vaccines (Basel) 6:E47. https://doi.org/10.3390/vaccines6030047.
32. Pardi N, Hogan MJ, Naradikian MS, Parkhouse K, Cain DW, Jones L, Moody MA, Verkerke HP, Myles A, Willis E, LaBranche CC, Montefiori DC, Lobby JL, Saunders KO, Liao HX, Korber BT, Sutherland LL, Scearce RM, Hraber PT, Tombacz I, Muramatsu H, Ni H, Balikov DA, Li C, Mui BL, Tam YK, Krammer F, Kariko K, Polacino P, Eisenlohr LC, Madden TD, Hope MJ, Lewis MG, Lee KK, Hu SL, Hensley SE, Cancro MP, Haynes BF, Weissman D. 2018. Nucleoside-modified mRNA vaccines induce potent T follicular helper and germinal center B cell responses. J Exp Med 215:1571–1588. https://doi.org/10.1084/jem.20171450.
33. Hai R, Krammer F, Tan GS, Pica N, Eggink D, Maamary J, Margine I, Albrecht RA, Palese P. 2012. Influenza viruses expressing chimeric hemagglutinins: globular head and stalk domains derived from different subtypes. J Virol 86:5774–5781. https://doi.org/10.1128/JVI.00137-12.
34. Steel J, Lowen AC, Wang TT, Yondola M, Gao Q, Haye K, Garcia-Sastre A, Palese P. 2010. Influenza virus vaccine based on the conserved hemagglutinin stalk domain. mBio 1:e00018-10. https://doi.org/10.1128/mBio.00018-10.
35. Impagliazzo A, Milder F, Kuipers H, Wagner MV, Zhu X, Hoffman RMB, van Meersbergen R, Huizingh J, Wanningen P, Verspuij J, de Man M, Ding Z, Apetri A, Kükrer B, Sneekes-Vriese E, Tomkiewicz D, Laursen NS, Lee PS, Zakrzewska A, Dekking L, Tolboom J, Tettero L, van Meerten S, Yu W, Koudstaal W, Goudsmit J, Ward AB, Meijberg W, Wilson IA, Radošević K. 2015. A stable trimeric influenza hemagglutinin stem as a broadly protective immunogen. Science 349:1301–1306. https://doi.org/10.1126/science.aac7263.
36. Park JK, Han A, Czajkowski L, Reed S, Athota R, Bristol T, Rosas LA, Cervantes-Medina A, Taubenberger JK, Memoli MJ. 2018. Evaluation of preexisting anti-hemagglutinin stalk antibody as a correlate of protection in a healthy volunteer challenge with influenza A/H1N1pdm virus. mBio 9:e02284-17. https://doi.org/10.1128/mBio.02284-17.
37. Memoli MJ, Czajkowski L, Reed S, Athota R, Bristol T, Proudfoot K, Fargis S, Stein M, Dunfee RL, Shaw PA, Davey RT, Taubenberger JK. 2015. Validation of the wild-type influenza A human challenge model H1N1pdMIST: an A(H1N1)pdm09 dose-finding investigational new drug study. Clin Infect Dis 60:693–702. https://doi.org/10.1093/cid/ciu924.
38. Darton TC, Blohmke CJ, Moorthy VS, Altmann DM, Hayden FG, Clutterbuck EA, Levine MM, Hill AV, Pollard AJ. 2015. Design, recruitment, and microbiological considerations in human challenge studies. Lancet Infect Dis 15:840–851. https://doi.org/10.1016/S1473-3099(15)00068-7.
39. Killingley B, Enstone JE, Greatorex J, Gilbert AS, Lambkin-Williams R, Cauchemez S, Katz JM, Booy R, Hayward A, Oxford J, Bridges CB, Ferguson NM, Nguyen Van-Tam JS. 2012. Use of a human influenza challenge model to assess person-to-person transmission: proof-of-concept study. J Infect Dis 205:35–43. https://doi.org/10.1093/infdis/jir701.
40. Balasingam S, Wilder-Smith A. 2016. Randomized controlled trials for influenza drugs and vaccines: a review of controlled human infection studies. Int J Infect Dis 49:18–29. https://doi.org/10.1016/j.ijid.2016.05.013.
41. Christensen SR, Toulmin SA, Griesman T, Lamerato LE, Petrie JG, Martin ET, Monto AS, Hensley SE. 2019. Assessing the protective potential of H1N1 influenza virus hemagglutinin head and stalk antibodies in humans. bioRxiv https://doi.org/10.1101/478222.
42. Petrie JG, Martin ET, Truscon R, Johnson E, Cheng CK, McSpadden E, Malosh RE, Lauring AS, Lamerato LE, Eichelberger MC, Ferdinands JM, Monto AS. 2018. Evaluation of correlates of protection against influenza A(H3N2) and A(H1N1)pdm09 infection: applications to the hospitalized patient population. bioRxiv https://doi.org/10.1101/416628.
43. Francis T. 1947. Dissociation of hemagglutinating and antibody-measuring capacities of influenza virus. J Exp Med 85:1–7.
44. Hirst GK. 1942. The quantitative determination of influenza virus and antibodies by means of red cell agglutination. J Exp Med 75:49–64. https://doi.org/10.1084/jem.75.1.49.
45. Hobson D, Curry RL, Beare AS, Ward-Gardner A. 1972. The role of serum haemagglutination-inhibiting antibody in protection against challenge infection with influenza A2 and B viruses. J Hyg 70:767–777. https://doi.org/10.1017/S0022172400022610.
46. Margine I, Palese P, Krammer F. 2013. Expression of functional recombinant hemagglutinin and neuraminidase proteins from the novel H7N9 influenza virus using the baculovirus expression system. J Vis Exp 81:e51112. https://doi.org/10.3791/51112:e51112.
47. Dreyfus C, Laursen NS, Kwaks T, Zuijdgeest D, Khayat R, Ekiert DC, Lee JH, Metlagel Z, Bujny MV, Jongeneelen M, van der Vlugt R, Lamrani M, Korse

HJ, Geelen E, Sahin O, Sieuwerts M, Brakenhoff JP, Vogels R, Li OT, Poon LL, Peiris M, Koudstaal W, Ward AB, Wilson IA, Goudsmit J, Friesen RH. 2012. Highly conserved protective epitopes on influenza B viruses. Science 337:1343–1348. https://doi.org/10.1126/science.1222908.
48. Ekiert DC, Bhabha G, Elsliger MA, Friesen RH, Jongeneelen M, Throsby M, Goudsmit J, Wilson IA. 2009. Antibody recognition of a highly conserved influenza virus epitope. Science 324:246–251. https://doi.org/10.1126/science.1171491.
49. DiLillo DJ, Tan GS, Palese P, Ravetch JV. 2014. Broadly neutralizing hemagglutinin stalk-specific antibodies require FcgammaR interactions for protection against influenza virus in vivo. Nat Med 20:143–151. https://doi.org/10.1038/nm.3443.
50. Vidarsson G, Dekkers G, Rispens T. 2014. IgG subclasses and allotypes: from structure to effector functions. Front Immunol 5:520. https://doi.org/10.3389/fimmu.2014.00520.
51. Nachbagauer R, Choi A, Izikson R, Cox MM, Palese P, Krammer F. 2016. Age dependence and isotype specificity of influenza virus hemagglutinin stalk-reactive antibodies in humans. mBio 7:e01996. https://doi.org/10.1128/mBio.01996-15.
52. Pedersen GK, Hoschler K, Oie Solbak SM, Bredholt G, Pathirana RD, Afsar A, Breakwell L, Nostbakken JK, Raae AJ, Brokstad KA, Sjursen H, Zambon M, Cox RJ. 2014. Serum IgG titres, but not avidity, correlates with neutralizing antibody response after H5N1 vaccination. Vaccine 32:4550–4557. https://doi.org/10.1016/j.vaccine.2014.06.009.
53. Fu Y, Zhang Z, Sheehan J, Avnir Y, Ridenour C, Sachnik T, Sun J, Hossain MJ, Chen LM, Zhu Q, Donis RO, Marasco WA. 2016. A broadly neutralizing anti-influenza antibody reveals ongoing capacity of haemagglutinin-specific memory B cells to evolve. Nat Commun 7:12780. https://doi.org/10.1038/ncomms12780.
54. Sutton TC, Lamirande EW, Bock KW, Moore IN, Koudstaal W, Rehman M, Weverling GJ, Goudsmit J, Subbarao K. 2017. In vitro neutralization is not predictive of prophylactic efficacy of broadly neutralizing monoclonal antibodies CR6261 and CR9114 against lethal H2 influenza virus challenge in mice. J Virol 91:e01603-17. https://doi.org/10.1128/JVI.01603-17.
55. Seibert CW, Rahmat S, Krause JC, Eggink D, Albrecht RA, Goff PH, Krammer F, Duty JA, Bouvier NM, Garcia-Sastre A, Palese P. 2013. Recombinant IgA is sufficient to prevent influenza virus transmission in guinea pigs. J Virol 87:7793–7804. https://doi.org/10.1128/JVI.00979-13.
56. Muramatsu M, Yoshida R, Yokoyama A, Miyamoto H, Kajihara M, Maruyama J, Nao N, Manzoor R, Takada A. 2014. Comparison of antiviral activity between IgA and IgG specific to influenza virus hemagglutinin: increased potential of IgA for heterosubtypic immunity. PLoS One 9:e85582. https://doi.org/10.1371/journal.pone.0085582.
57. He W, Mullarkey CE, Duty JA, Moran TM, Palese P, Miller MS. 2015. Broadly neutralizing anti-influenza virus antibodies: enhancement of neutralizing potency in polyclonal mixtures and IgA backbones. J Virol 89:3610–3618. https://doi.org/10.1128/JVI.03099-14.
58. Kirchenbaum GA, Ross TM. 2014. Eliciting broadly protective antibody responses against influenza. Curr Opin Immunol 28:71–76. https://doi.org/10.1016/j.coi.2014.02.005.
59. Sautto GA, Kirchenbaum GA, Ross TM. 2018. Towards a universal influenza vaccine: different approaches for one goal. Virol J 15:17. https://doi.org/10.1186/s12985-017-0918-y.
60. Schmitz N, Beerli RR, Bauer M, Jegerlehner A, Dietmeier K, Maudrich M, Pumpens P, Saudan P, Bachmann MF. 2012. Universal vaccine against influenza virus: linking TLR signaling to anti-viral protection. Eur J Immunol 42:863–869. https://doi.org/10.1002/eji.201041225.
61. Bloom JD, Gong LI, Baltimore D. 2010. Permissive secondary mutations enable the evolution of influenza oseltamivir resistance. Science 328:1272–1275. https://doi.org/10.1126/science.1187816.
62. Alter G, Malenfant JM, Altfeld M. 2004. CD107a as a functional marker for the identification of natural killer cell activity. J Immunol Methods 294:15–22. https://doi.org/10.1016/j.jim.2004.08.008.
63. Smith P, DiLillo DJ, Bournazos S, Li F, Ravetch JV. 2012. Mouse model recapitulating human Fcgamma receptor structural and functional diversity. Proc Natl Acad Sci U S A 109:6181–6186. https://doi.org/10.1073/pnas.1203954109.
64. Monto AS, Petrie JG, Cross RT, Johnson E, Liu M, Zhong W, Levine M, Katz JM, Ohmit SE. 2015. Antibody to influenza virus neuraminidase: an independent correlate of protection. J Infect Dis 212:1191–1199. https://doi.org/10.1093/infdis/jiv195.
65. Mullarkey CE, Bailey MJ, Golubeva DA, Tan GS, Nachbagauer R, He W, Novakowski KE, Bowdish DM, Miller MS, Palese P. 2016. Broadly neutralizing hemagglutinin stalk-specific antibodies induce potent phagocytosis of immune complexes by neutrophils in an Fc-dependent manner. mBio 7:e01624-16. https://doi.org/10.1128/mBio.01624-16.
66. World Health Organization. 2011. Manual for the laboratory diagnosis and virological surveillance of influenza. World Health Organization, Geneva, Switzerland.
67. Nachbagauer R, Shore D, Yang H, Johnson SK, Gabbard JD, Tompkins SM, Wrammert J, Wilson PC, Stevens J, Ahmed R, Krammer F, Ellebedy AH. 2018. Broadly-reactive human monoclonal antibodies elicited following pandemic H1N1 influenza virus exposure protect mice from highly pathogenic H5N1 challenge. J Virol 92:e00949-18. https://doi.org/10.1128/JVI.00949-18.
68. Hoffmann E, Neumann G, Kawaoka Y, Hobom G, Webster RG. 2000. A DNA transfection system for generation of influenza A virus from eight plasmids. Proc Natl Acad Sci U S A 97:6108–6113. https://doi.org/10.1073/pnas.100133697.